INTERNATIONAL JOURNAL OF PHARMACEUTICAL SCIENCES
[ISSN: 0975-4725; CODEN(USA): IJPS00]
Journal Homepage: https://www.ijpsjournal.com

OPEN ACCESS

Research Article

Development of 3D Printed Variable Dose Multi-Drug Tablets Containing Metformin, Sitagliptin, and Simvastatin by Selective Laser Sintering and their Simultaneous Quantification Using a Novel HPLC Method

Sanjaykumar Gayakwad*[1], Alisha Patel[1,2]

[1] *Department of Pharmaceutical Sciences, School of Pharmacy, Massachusetts College of Pharmacy, Boston, MA, USA, 02115*
[2] *Oddity Labs, Cambridge, MA, USA 02142l.*

ARTICLE INFO

Published: 04 Aug 2026
Keywords:
Selective laser sintering, 3D printing, Personalized medicine, Fixed-dose combination, Hypertension, Valsartan, Hydrochlorothiazide, Amlodipine besylate
DOI:
10.5281/zenodo.21800558

ABSTRACT

Personalized medicine offers an opportunity to improve hypertension management through patient-specific drug combinations and dose strengths while reducing pill burden and enhancing medication adherence. This study aimed to develop and evaluate selective laser sintering (SLS)-based 3D-printed variable-dose combination tablets containing hydrochlorothiazide, valsartan, and amlodipine besylate, and to develop a novel HPLC method for their simultaneous quantification. Drug–excipient compatibility was assessed using differential scanning calorimetry (DSC) and thermogravimetric analysis (TGA). A gradient HPLC method was developed and validated for simultaneous analysis of the three drugs. Powder blends containing Kollidon® VA 64, crospovidone, and FD&C Red Dye No. 3 were processed using SLS 3D printing, and critical process parameters were optimized. Two 3D-printed formulations (F17 and F22) and three conventionally compressed formulations (F23–F25) were evaluated for drug content and dissolution performance. Compatibility studies identified mannitol as incompatible with hydrochlorothiazide and amlodipine besylate, while all other excipients were suitable for formulation development. The developed HPLC method successfully separated hydrochlorothiazide, valsartan, and amlodipine besylate with retention times of 6.6, 2.3, and 9.9 min, respectively. Optimized printing conditions consisted of a chamber temperature of 65°C, surface temperature of 95°C, 5% FD&C Red Dye No. 3, and 5% crospovidone. Drug-content analysis demonstrated acceptable assay values for all formulations. F17 exhibited 60-min drug releases of 70.9% hydrochlorothiazide, 92.8% valsartan, and 60.0%

***Corresponding Author:** Sanjaykumar Gayakwad
Address: *School of Pharmacy, Massachusetts College of Pharmacy, Boston, MA, USA, 02115.*
Email : sanjaykumar.gayakwad@mcphs.edu

Relevant conflicts of interest/financial disclosures: The authors declare that the research was conducted in the absence of any commercial or financial relationships that could be construed as a potential conflict of interest.

amlodipine besylate, whereas F22 showed lower releases of 40.5%, 49.0%, and 30.5%, respectively. Comparative studies with compressed tablets suggested that polymer–drug fusion and potential dye-related interactions influenced dissolution behavior. These findings demonstrate the feasibility of SLS 3D printing for the fabrication of personalized multidrug antihypertensive tablets.

INTRODUCTION

Hypertension remains one of the most prevalent chronic non-communicable diseases worldwide and is a major contributor to cardiovascular morbidity and mortality. Sustained elevation of blood pressure induces structural and functional alterations in the vasculature, including arterial stiffening and reduced vascular elasticity, which ultimately compromises tissue perfusion and organ function [1]. The increased hemodynamic load forces the heart to work against elevated vascular resistance, resulting in left ventricular hypertrophy, myocardial ischemia, angina, and, over time, heart failure. In addition to cardiovascular complications, hypertension is a leading cause of chronic kidney disease, while diabetic patients are particularly susceptible to the development of hypertension and its associated complications [2, 3].

Despite the availability of numerous antihypertensive therapies, approximately 70% of patients fail to achieve the recommended target blood pressure of <140/90 mmHg with monotherapy [4]. Long-term studies indicate that most patients require an average of three antihypertensive agents to attain adequate blood pressure control [5]. Because hypertension is driven by multiple physiological pathways, combination therapy offers greater efficacy than monotherapy by targeting several mechanisms simultaneously [5, 6]. However, treatment adherence remains a major challenge, particularly in patients with multiple comorbidities and complex medication regimens [7]. Single-pill combination therapies have therefore emerged as an important strategy to reduce pill burden and improve adherence [5].

Current first-line antihypertensive treatment relies primarily on calcium channel blockers (CCBs), angiotensin-converting enzyme (ACE) inhibitors or angiotensin receptor blockers (ARBs), and diuretics [6,8,9]. Clinical evidence demonstrates that combining antihypertensive agents from complementary pharmacological classes produces substantially greater blood pressure reductions than escalating the dose of a single agent, while reducing dose-related adverse effects [10, 11]. Consequently, fixed-dose combinations (FDCs) and single-pill combinations (SPCs) have become widely accepted therapeutic approaches for hypertension management [12]. Examples include ARB/diuretic combinations, which counteract compensatory activation of the renin–angiotensin system and reduce diuretic-associated hypokalemia [13-15], and ARB/CCB or ACE inhibitor/CCB combinations, which improve cardiovascular outcomes while minimizing CCB-induced peripheral edema [16, 17].

Although commercially available FDCs provide important benefits, they are inherently limited by their fixed strengths and compositions. These products are designed for average patient populations and therefore provide limited flexibility for individualized dose adjustment according to patient-specific characteristics, disease severity, treatment response, and comorbidities [18]. Such limitations highlight the growing need for precision medicine approaches that tailor pharmacotherapy to individual patient requirements.

Precision medicine seeks to optimize therapeutic outcomes by integrating patient-specific factors, including genetics, disease characteristics, lifestyle, and environmental influences, into

clinical decision-making [19, 20]. In hypertension management, this approach creates opportunities to customize drug combinations, doses, and release profiles according to individual therapeutic needs [21]. Conventional pharmaceutical manufacturing, however, is poorly suited to produce personalized dosage forms on demand. Traditional dose-adjustment strategies such as tablet splitting often result in significant variability in tablet mass and drug content, thereby compromising dosing accuracy and therapeutic reliability [5, 22-24]. For precision medicine to be effective, the tablets need to be easily fabricated, customizable, and highly affordable which would encourage widespread usage and allow it to be fabricated on the spot after diagnosis. [22].

Three-dimensional (3D) printing has emerged as a transformative technology capable of addressing these challenges by enabling the fabrication of patient-specific dosage forms directly from digital designs [5, 25, 26]. Through precise control of tablet geometry, drug loading, and internal structure, 3D printing facilitates the production of individualized medicines with tailored drug release profiles and multidrug combinations. Such personalized polypills have the potential to improve medication adherence, reduce pill burden, minimize adverse effects, and enhance therapeutic outcomes in patients with hypertension [27-29]. Several 3D-printing technologies have been explored for pharmaceutical applications, including fused deposition modeling (FDM), binder jetting, stereolithography (SLA), semi-solid extrusion, and selective laser sintering (SLS) [25, 26, 30]. However, FDM often requires high processing temperatures and drug-loaded filament preparation, potentially limiting the incorporation of thermosensitive drugs. Binder jetting requires liquid binders and additional post-processing steps, while SLA depends on photopolymerizable materials that may present formulation and regulatory challenges [25, 26, 30]. Among these technologies, Selective Laser Sintering (SLS) offers several distinct advantages for the fabrication of personalized multidrug tablets. SLS employs a laser to selectively fuse powder particles in a layer-by-layer manner, enabling the production of dosage forms with high precision, excellent reproducibility, and complex internal architectures. Unlike FDM, SLS does not require filament preparation, thereby simplifying formulation development and expanding the range of compatible pharmaceutical excipients. The technology also enables precise modulation of tablet porosity, density, drug loading, and release behavior while minimizing material waste and supporting rapid, small-batch production [25, 26, 30]. In addition, its solvent-free process and ability to incorporate multiple active pharmaceutical ingredients (APIs) within a single dosage form make SLS particularly suitable for the development of personalized antihypertensive polypills. The ability of SLS technology to produce individualized combination products directly addresses one of the major shortcomings of conventional FDCs: the lack of dosing flexibility. For hypertensive patients requiring multiple agents at personalized dose strengths, SLS provides a practical platform for the on-demand manufacture of patient-centric dosage forms that align with the principles of precision medicine [19-21].

Despite the growing interest in pharmaceutical 3D printing and the demonstrated clinical benefits of antihypertensive combination therapy, the integration of these two fields remains largely unexplored. Most reported studies on 3D-printed oral dosage forms have focused on single-drug systems or proof-of-concept formulations, whereas relatively few investigations have addressed the development of personalized multidrug antihypertensive tablets capable of

simultaneously delivering clinically relevant drug combinations at individualized dose strengths. Furthermore, although Selective Laser Sintering (SLS) has emerged as a promising platform for manufacturing highly customizable solid dosage forms, limited information is available regarding its application for producing patient-centric antihypertensive polypills that combine the therapeutic advantages of fixed-dose combinations with the flexibility required for precision medicine. Consequently, a significant gap exists between the clinical demand for individualized antihypertensive therapies and the availability of robust manufacturing approaches capable of delivering customized multidrug dosage forms in a practical and scalable manner. Addressing this gap is essential for translating the concept of precision cardiovascular pharmacotherapy from a theoretical framework into a clinically applicable reality.

Thus, the rationale of the present study is to integrate the established clinical benefits of antihypertensive combination therapy with the flexibility of personalized medicine through the application of selective laser sintering based 3D printing technology. SLS was selected because of its high resolution, formulation versatility, solvent-free processing, compatibility with multiple APIs, and suitability for small-scale, on-demand pharmaceutical manufacturing. The objective of this study is to develop and evaluate personalized multidrug antihypertensive tablets fabricated using SLS 3D printing, thereby establishing a platform for next-generation patient-centric management of hypertension.

MATERIALS AND METHODS

Materials

Valsartan, hydrochlorothiazide, and amlodipine besylate were purchased from Biosynth International, Inc. (KY, USA). Kollidon VA 64 and Kollidon VA 64 fine were obtained from BASF Corporation (NY, USA). Crospovidone, microcrystalline cellulose (MCC), sodium starch glycolate, and croscarmellose sodium were obtained from JRS Pharma (NY, USA). Mannitol, polyethylene oxide, ammonium acetate, FD&C Red #3, FD&C Red #40, FD&C Yellow #6, and FD&C Blue #3 were purchased from Fischer Scientific (MA, USA). Acetonitrile (HPLC grade), and methanol (HPLC grade) was purchased from VWR International (PA, USA). Candurin® Gold Sheen was provided as a free sample by EMD Performance Materials Corp. (Germany).

Excipient Compatibility

Physical mixtures of valsartan, hydrochlorothiazide, amlodipine besylate, and excipients were prepared in a 1:1 ratio, mixed for 5 minutes in a mortar and pestle to ensure homogeneity, and 5–10 mg samples were subjected to differential scanning calorimetry (DSC) and thermogravimetric analysis (TGA). DSC was performed using DSC25 (TA Instruments) where samples (5–10 mg) were placed in T_0 aluminum pans, sealed, and heated at 10°C/min under a nitrogen purge (50 mL/min) from 25°C to 400°C. Thermograms were analyzed for melting or decomposition onset using TRIOS software. TGA (TGA55, TA Instruments) was conducted on 5–10 mg samples in aluminum crucibles, heated at 10°C/min under a nitrogen purge (50 mL/min) from 25°C to 400°C. Thermal degradation profiles were analyzed using TRIOS software.

Simultaneous Determination of Valsartan, Hydrochlorothiazide, Amlodipine besylate

A comprehensive review of the literature revealed several reported high-performance liquid chromatography (HPLC) methods for the quantitative determination of amlodipine, valsartan, and hydrochlorothiazide, either as individual drug substances or in various fixed-dose combination products [31-36]. However, differences in chromatographic conditions, analytical objectives, and formulation characteristics necessitated the development of a robust method capable of the simultaneous determination of all three drugs in the present study.

Chromatographic analyses were performed using a Waters e2695 HPLC system (Waters Corporation, Milford, MA, USA) equipped with a 2489 UV/Visible detector and controlled through Empower™ chromatography software. Analytical-grade ammonium acetate, acetonitrile, and methanol were used throughout the study. All reagents and solvents employed for method development and validation were of analytical grade. Method development was conducted through a systematic optimization process to achieve satisfactory separation, peak symmetry, and resolution of hydrochlorothiazide, valsartan, and amlodipine besylate. Several chromatographic parameters were investigated, including the composition of the mobile phase, the ratio of organic solvent to aqueous buffer, and other chromatographic conditions such as flow rate, detection wavelength, and column operating conditions. Multiple experimental trials were performed to identify the optimal conditions that provided adequate retention, high resolution, and reproducible peak characteristics for all analytes. Finally, chromatographic separation was achieved on a Phenomenex Luna C18(2) 100 Å column (Phenomenex, Torrance, CA, USA, 150 x 4.6 mm, 5 µm) maintained at 30 ^{0}C. The mobile phase consisted of ammonium acetate buffer (30 mM, neutral pH, solution A) and a mixture of methanol and acetonitrile in the volume ratio of 80:20 (solution B) with a flow rate of 1.2 mL/min and injection volume of 10 µL. Detection was performed at 235 nm. Following optimization, a gradient elution method (Table 1) suitable for the simultaneous determination of hydrochlorothiazide, valsartan, and amlodipine besylate was established and subsequently validated.

Standard solutions were prepared by dissolving 5 mg of each drug in 10 mL of diluent (mixture of methanol and ammonium acetate buffer with volume ratio of 70:30), followed by serial dilutions to obtain 100 µg/mL stock solution of each drug. Accurately measured aliquots from the stock standard solutions of valsartan, hydrochlorothiazide and amlodipine besylate were transferred into sets of 10 mL volumetric flasks and diluted to volume with the diluent to prepare concentration ranges of 1.56 – 100 µg/mL. Concentration values were then plotted against area under the peak (AUP) values. Mobile phase A was prepared by dissolving 2.31 g of ammonium acetate (30mM) in 1000 mL deionized water. Solution was then filtered with 0.45 µm membrane filter (MilliporeSigma, MA, USA).

Table 1 Gradient flow conditions for the optimized HPLC method

Time (min)	Mobile phase A (% v/v)	Mobile phase B (% v/v)
0 – 2	70	30
2 – 4	70	30
4 – 10	40	60
10 – 12	40	60
12 – 14	70	30
14 – 16	70	30

3D Printing of Placebo Tablets

Powder blends were prepared by individually passing all formulation components through a #40 mesh sieve to ensure uniform particle size

distribution. The sieved materials were then blended manually using a mortar and pestle until a homogeneous mixture was obtained. The resulting powder blend was subsequently re-sieved through a #40 mesh to break down any agglomerates formed during mixing and to further improve blend uniformity, which is critical for consistent powder spreading and processing during Selective Laser Sintering (SLS) 3D printing. All formulation constituents were incorporated based on their respective % w/w composition.

Placebo formulations containing Kollidon® VA 64 (70–80% w/w), Kollidon® VA 64 Fine (5–15% w/w), Crospovidone (3% w/w), and different colorants, including FD&C Red #3, FD&C Red #40, FD&C Yellow #6, FD&C Blue #3, and Candurin® Gold Sheen, were evaluated for their suitability in SLS based 3D printing. Crospovidone was incorporated as a superdisintegrant to promote rapid tablet disintegration, while the colorants were included as laser energy absorbers to enhance the sintering process. Among the various formulations investigated, the formulation composition shown in Table 2, containing Kollidon® VA 64 (80% w/w), Kollidon® VA 64 Fine (13% w/w), FD&C Red #3 (5% w/w), and Crospovidone (3% w/w) demonstrated the most favorable printing performance and tablet characteristics.

Table 2 Final formulation composition for placebo tablets

Ingredient	Composition (% w/w)	mg/ tablet
Kollidon® VA64	80	200.0
Kollidon® VA 64 Fine	12	30.0
Crospovidone	3	7.5
FD&C Red #3	5	12.5
Total	100	250.0

Tablet designs (10 mm diameter × 5 mm height) were created using Tinkercad® software and exported as stereolithography (.STL) files to Sintratec Central. A 150 g powder batch of the optimized formulation (Table 2) was prepared and loaded into SLS 3D printer reservoir (Sintratec Kit, 3D Chimera, Miami, FL, USA). Prior to printing, the powder bed was preheated to facilitate the sintering process. Printing parameters were optimized by evaluating chamber and powder surface temperatures ranging from 80°C to 110°C and laser scanning speeds between 150 and 300 mm/s. Following optimization, powder surface and chamber temperatures were set at 110 °C and 95 °C respectively. Laser scanning speed of 150 mm/s was found to be most suitable. After printing, the tablets were allowed to cool for 30–45 min before removal from the powder bed and recovery of the printed tablets by removing excess unsintered powder. Average tablet weight was determined using an electronic analytical balance, while tablet diameter and thickness were measured using a digital vernier caliper. The 3D printed placebo tablets were stored at room temperature in scintillation vials for further evaluation.

3D Printing of Multi-Drug Combination Tablets

Multi-drug combination tablets were fabricated using optimized process parameters established for placebo formulations. Formulations containing lower doses (F1) and higher doses (F2) shown in Table 3, respectively were designed based on the minimum dose requirements of the three drugs [37-40].

Table 3 Formulation composition of the 3D printed multi-drug tablets

Formulation	Kollidon VA 64 (% w/w)	Crospovidone (% w/w)	Dye (% w/w)	Chamber temperature	Surface temperature
F11	71.0	3.0	5	95°C	110°C
F12	71.0	3.0	5	75°C	90°C
F13	71.0	3.0	5	65°C	95°C

F14	74.0	3.0	2	65°C	95°C
F15	73.0	3.0	3	65°C	95°C
F16	72.0	3.0	4	65°C	95°C
F17	69.0	5.0	5	65°C	95°C
F21	63.5	5.0	5	65°C	95°C
F22	61.0	7.5	5	65°C	90°C

The F1 series comprised 12.5 mg hydrochlorothiazide, 40 mg valsartan and 5 mg amlodipine besylate with tablet dimensions of 10 mm x 5 mm to yield tablets with a target weight of 280 mg. The F2 series comprised of 12.5 mg hydrochlorothiazide, 80 mg valsartan and 5 mg amlodipine besylate with the tablet dimensions of 12 mm x 6 mm to accommodate the higher dose of valsartan and yield tablets with a target weight of 380 mg. Powder blends (200 g) containing drugs and excipients were mixed in a mortar and pestle, followed by sieving through a #40 mesh and re-mixing to ensure homogeneity. The prepared blends were processed using the same SLS printer (Sintratec Kit, 3D Chimera). Cylindrical printlets were designed in Tinkercad and exported as .stl files to Sintratec Central. 3D printed multi-drug tablets were stored at room temperature in scintillation vials for further evaluation.

Preparation of Multi-Drug Combination Tablets by Compression

Single punched compressed tablets were prepared for F2 series containing 12.5 mg hydrochlorothiazide, 5.0 mg amlodipine besylate and a higher dose (80 mg) of valsartan. Formulation ingredients for F23 were kept identical with that of formulation F22 (3D printed formulation). Formulation F24 did not contain the dye while F25 included microcrystalline cellulose and sucrose as diluents. The target tablet weight was set at 380 mg. Desired quantities of drugs and excipients (as per the composition shown in Table 4) were accurately weighed and blended using a mortar and pestle to prepare a batch size of 10 g. The powder blend was passed through a #40 mesh sieve and re-mixed to ensure content uniformity. Appropriate amounts of the final blend, corresponding to the target tablet weight, were then compressed at 1000 psi into tablets using a single-punch tablet press (Enerpac Model MTC M-1, GlobePharma, NJ, USA). Compressed multi-drug tablets were stored at room temperature in scintillation vials for further evaluation.

Table 4 Formulation composition of single punch compressed multi-drug tablets

Formulation	Dye (%w/w)	Crospovidone (%w/w)	Kollidon VA 64 (%w/w)	MCC (%w/w)	Sucrose (%w/w)
F23	5	7.5	61	-	-
F24	-	7.5	66.8	-	-
F25	5	7.5	11.8	35	15

Drug Content Determination

For quantification of the drug in the prepared tablets, three tablets were individually weighed on an analytical balance (OHAUS Explorer E1140, Ohaus Corporation, Parsippany, NJ, USA) and crushed. Entire crushed powder from each tablet was then dissolved in 200 mL of diluent (mixture of methanol and ammonium acetate buffer with volume ratio of 70:30) sonicated for 30 minutes, filtered (0.45 μm), and analyzed by the developed HPLC method.

Drug Dissolution

Drug release profiles of 3D printed and compressed tablets were tested using USP Dissolution apparatus Type – II (Distek, North Brunswick, NJ, USA). Each vessel (n = 6) contained 900 mL of 10mM sodium phosphate buffer solution (pH 6.8) as listed in the USP monograph [40]. Paddle speed was fixed at 100 rpm and the buffer temperature was maintained at 37 ± 0.5°C. Samples (6 mL) were withdrawn at different time intervals and filtered through 0.45 µm membrane filters and immediately replaced with fresh buffer. Drug concentrations were simultaneously determined using the previously validated HPLC method.

Statistical Analysis

The data was represented as mean values along with the standard deviation (SD). The one-way ANOVA test determined statistical significance, with the probability value (p) set at < 0.05 indicating significance. The GraphPad Prism 8 software was used to perform the analysis of variance (ANOVA).

RESULTS

Excipient Compatibility

The DSC thermogram of pure valsartan exhibited a characteristic melting endotherm at approximately 97°C (Fig. 1, Insert A). To evaluate drug–excipient compatibility, physical mixtures of valsartan and each excipient were prepared in a 1:1 ratio and analyzed by DSC (Fig. 1). The excipients evaluated included sodium starch glycolate, croscarmellose sodium, crospovidone, microcrystalline cellulose, hydroxypropyl methylcellulose, mannitol, polyethylene oxide, and Kollidon® VA 64. The melting endotherm of valsartan was retained in all mixtures, with peak temperatures observed between 87°C and 95°C. The absence of any significant changes in the thermal behavior of valsartan suggested good compatibility between the drug and the tested excipients. The DSC thermogram of pure hydrochlorothiazide showed a sharp melting endotherm at approximately 272°C (Fig. 2, Insert A). Physical mixtures of hydrochlorothiazide with each excipient (1:1 ratio) were subsequently analyzed (Fig. 2). In most mixtures, the melting endotherm of hydrochlorothiazide was maintained within the range of 270–275°C, indicating compatibility with the excipients. However, in the hydrochlorothiazide–mannitol mixture, the characteristic melting endotherm of hydrochlorothiazide was not detected, suggesting a possible interaction between the drug and mannitol.

Similarly, pure amlodipine besylate exhibited a melting endotherm at approximately 207°C (Fig. 3, Insert A). DSC analysis of 1:1 physical mixtures of amlodipine besylate with the selected excipients was performed (Fig. 3). For most excipients, the melting endotherm remained within the range of 205–207°C, indicating compatibility. In contrast, the amlodipine besylate–mannitol mixture showed a marked shift in the melting endotherm, suggesting a potential drug–excipient interaction and possible incompatibility between amlodipine besylate and mannitol.

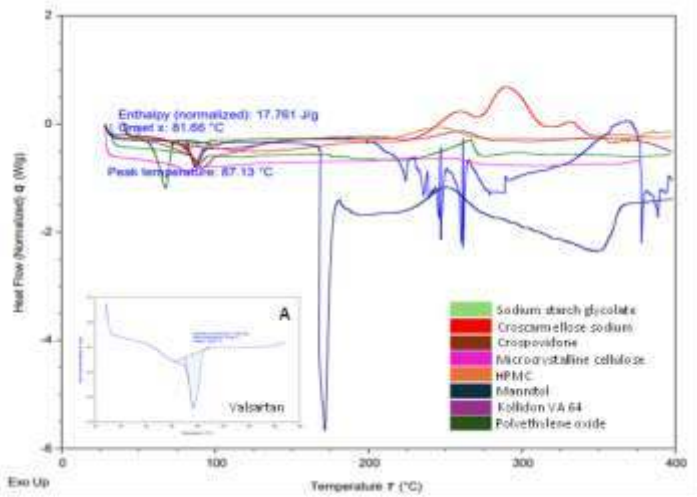

Figure 1 DSC thermograms showing compatibility of valsartan with various excipients, A) Melting endotherm of pure valsartan.

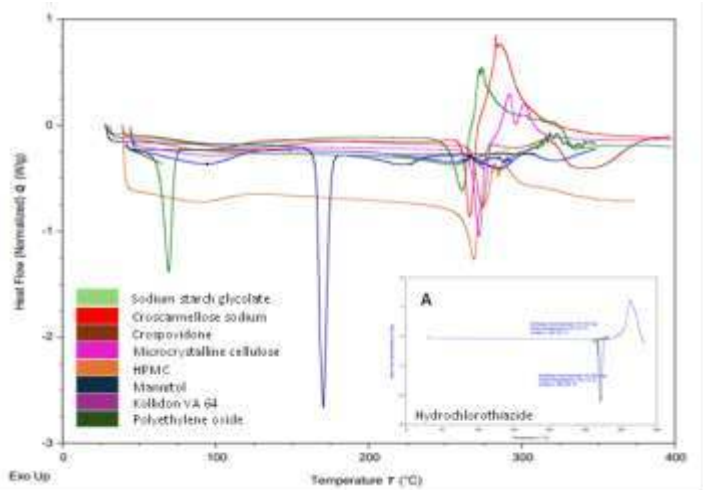

Figure 2 DSC thermograms showing compatibility of hydrochlorothiazide with various excipients, A) Melting endotherm of hydrochlorothiazide.

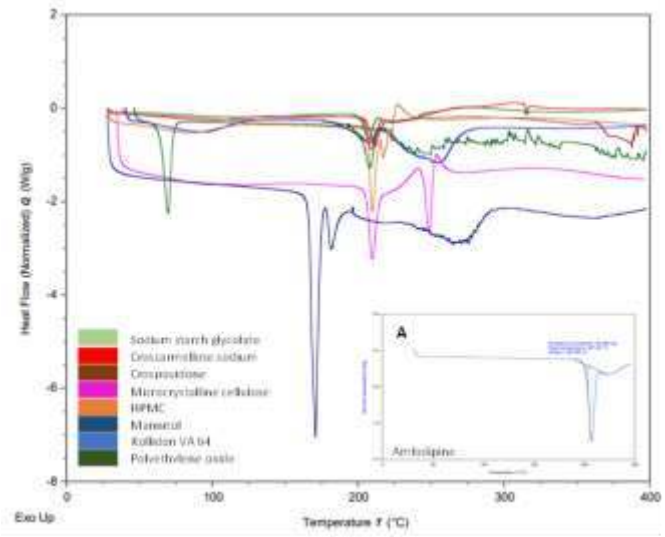

Figure 3 DSC thermograms showing compatibility of amlodipine besylate with various excipients, A) Melting endotherm of pure amlodipine besylate.

Thermal stability of the individual drugs was further evaluated using TGA. The TGA thermogram of valsartan (Fig. 4A) showed the onset of degradation at approximately 191°C, accompanied by an initial weight loss of 2.8%, likely due to the loss of residual moisture. A rapid and substantial weight loss of up to 95% was observed beyond 205°C, indicating extensive thermal degradation. Therefore, the degradation temperature of valsartan was considered to be approximately 191°C. For hydrochlorothiazide, TGA analysis (Fig. 4B) revealed the onset of degradation at approximately 267°C, accompanied by a significant weight loss of about 49%. This temperature was therefore identified as the degradation temperature of hydrochlorothiazide. The TGA thermogram of amlodipine besylate (Fig. 4C) showed the onset of degradation at approximately 177°C, with a corresponding weight loss of about 52%. Accordingly, 177°C was identified as the degradation temperature of amlodipine besylate. To support the optimization of the 3D printing process, 1 g of formulation F1a was prepared and subjected to DSC analysis. The thermogram showed an onset melting temperature of 73°C and a peak melting temperature of 88°C (Fig. 4D). These values were used as reference points for selecting appropriate chamber and surface temperatures during the subsequent printing of various formulations. Overall, DSC studies demonstrated compatibility of valsartan with all tested excipients, whereas potential incompatibilities were observed between mannitol and both hydrochlorothiazide and amlodipine besylate. TGA analysis established the thermal degradation temperatures of valsartan, hydrochlorothiazide, and amlodipine besylate as approximately 191°C, 267°C, and 177°C, respectively.

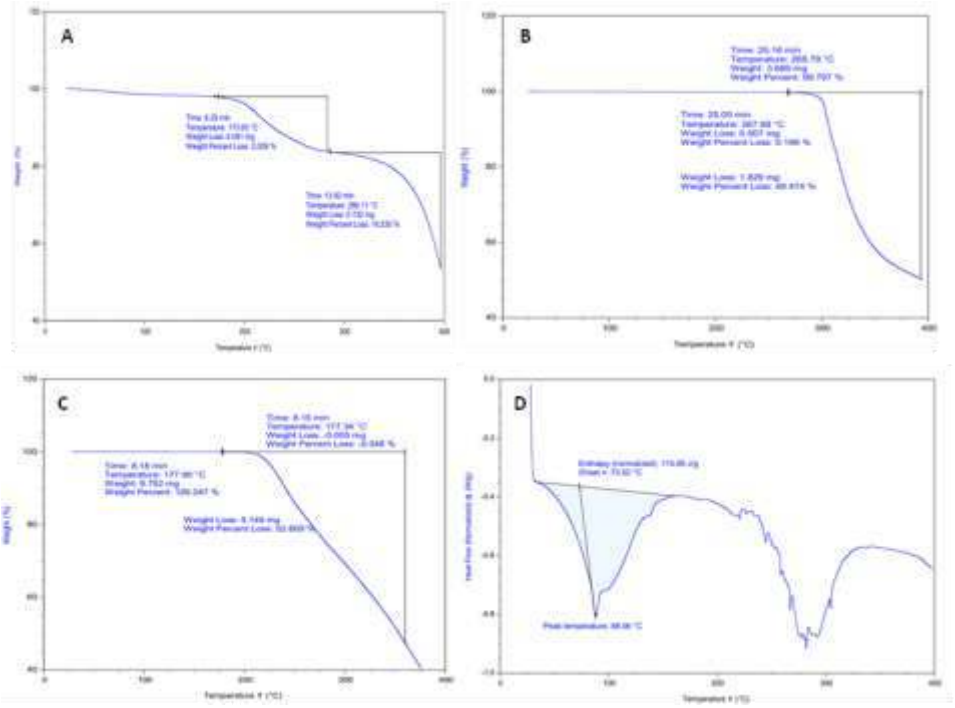

Figure 4 TGA graph of A) Valsartan, B) Hydrochlorothiazide, and C) Amlodipine besylate. D) DSC thermogram of formulation F11 showing onset of melting temperature at 73°C and a peak melting temperature of 88°C.

Simultaneous Determination of Valsartan, Hydrochlorothiazide, Amlodipine besylate

The HPLC method employing gradient elution was initially evaluated using individual drug

solutions. The retention times were found to be 2.36 min for valsartan, 6.77 min for hydrochlorothiazide, and 10.01 min for amlodipine besylate. Subsequently, a mixed standard containing all three drugs was analyzed to assess the method's ability to simultaneously separate the analytes. In the combined sample, retention times were recorded at 2.27 min for valsartan, 6.60 min for hydrochlorothiazide, and 9.87 min for amlodipine besylate. The chromatogram demonstrated well-resolved and distinct peaks for all three compounds, confirming good separation and the suitability of the method for simultaneous analysis (Fig. 5).

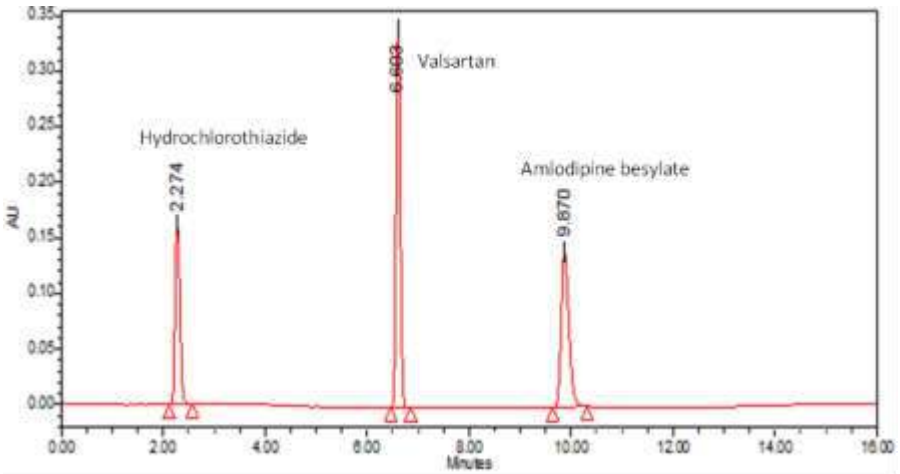

Figure 5 HPLC chromatogram of combination of hydrochlorothiazide, valsartan and amlodipine besylate at a wavelength of 235 nm and concentration of 100 µg/mL.

The developed method was further validated in accordance with analytical validation requirements. Linearity was evaluated through both intra-day and inter-day studies over a concentration range of 1.56–100 µg/mL for each drug. Calibration curves exhibited a strong linear relationship between peak area and concentration. The slope, correlation coefficient (R^2), and other statistical parameters, including standard deviation (SD), relative standard deviation (RSD), limit of detection (LOD), and limit of quantification (LOQ), were determined and are presented in Table 5. These results demonstrated the accuracy, precision, sensitivity, and reliability of the developed HPLC method for the simultaneous quantification of valsartan, hydrochlorothiazide, and amlodipine besylate.

Table 5 Linearity results for the developed HPLC method

Drug	Correlation Coefficient (R^2)	% RSD Intra-day	% RSD Inter-day	LOD (µg/mL)	LOQ (µg/mL)
Hydrochlorothiazide	0.99	1.06	1.84	0.89	2.69
Valsartan	1	0.75	2.43	0.88	1.99
Amlodipine besylate	1	0.95	2.50	1.02	3.09

3D Printed Placebo Tablets

Selective laser sintering (SLS) 3D printing requires excipients with suitable sintering characteristics and additives that enhance laser energy absorption to produce tablets with adequate mechanical strength [41]. Kollidon® VA64, a copolymer of N-vinylpyrrolidone and vinyl acetate (60:40), was selected due to its proven suitability for SLS printing and relatively low

glass transition temperature (~115°C), which facilitates efficient particle fusion [42-46].

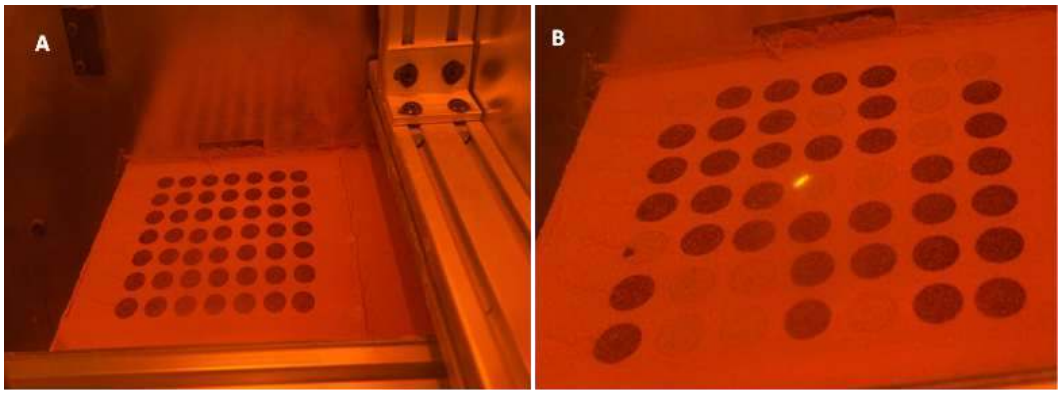

Figure 6 SLS based 3D printing process. A) Powder spreading via the coater, and B) Powder sintering via laser resulting in tablet formation.

To improve laser energy absorption, several colorant dyes were evaluated. FD&C Red #3 was identified as the most suitable dye, and a concentration of 3% (w/w) provided consistent print quality and acceptable mechanical properties. However, formulations containing only Kollidon® VA64 and dye exhibited poor disintegration. Therefore, crospovidone (5% w/w), a commonly used superdisintegrant, was incorporated to promote rapid tablet disintegration [47]. The final placebo formulation consisted of Kollidon® VA64, Kollidon® VA64 fine, crospovidone, and FD&C Red #3. Printing studies showed that laser scanning speed strongly influenced tablet formation. A scanning speed of 350 mm/s resulted in incomplete sintering and poorly formed printlets, whereas 150 mm/s produced well-sintered tablets with satisfactory mechanical integrity (Fig. 6). Optimal printing was achieved at a chamber temperature of 95°C and a surface temperature of 110°C. Under these conditions, the printed placebo tablets displayed consistent physical characteristics, with an average weight of 244.2 ± 14.0 mg (n = 10), diameter of 9.62 ± 0.20 mm, and height of 5.45 ± 0.15 mm, closely matching the target dimensions of 10 mm and 5 mm, respectively (Fig. 7).

3D Printed Multi-Drug Combination Tablets

Multi-drug tablets were initially prepared using formulation F11 under the printing conditions previously optimized for placebo tablets (chamber temperature: 95°C; surface temperature: 110°C). However, printing was unsuccessful because the formulation solidified at these elevated temperatures, preventing adequate spreading of the powder mixture across the printing platform and resulting in a printing failure.

Figure 7 SLS based 3D printed tablets. A) Placebo tablets, B) Tablets in a scintillation vial, and C) Diameter of tablets as measured by vernier calipers.

To better understand the thermal behavior of the formulation and optimize the printing conditions, differential scanning calorimetry (DSC) analysis was performed. As shown in Fig. 4D, the formulation exhibited an onset melting temperature of 73°C and a melting peak at 88°C. Based on these findings, the printing temperatures were reduced. For formulation F12, the chamber and surface temperatures were adjusted to 75°C and 90°C, respectively. Although printing progressed further under these conditions, the formulation solidified during the final stages of the process, leading to printing failure and indicating that additional optimization was required.

Further modification of the printing parameters was evaluated with formulation F13 by reducing the chamber temperature to 65°C and increasing the surface temperature to 95°C. These conditions resulted in successful tablet fabrication. Following cooling and powder recovery, the printed tablets were visually observed to be compact and intact, with no apparent powder loss during handling. The influence of dye concentration on tablet formation was subsequently investigated using formulations F14–F16, containing 2%, 3%, and 4% FD&C Red Dye #3, respectively, while maintaining the printing parameters established for F13. No intact tablets were recovered following printing of formulations F14 and F15. Although tablets were successfully recovered from formulation F16, they exhibited powder loss during handling, indicating insufficient interparticle binding. These findings suggest that a dye concentration of 5% is required to provide adequate binding and ensure successful tablet formation.

To improve tablet disintegration while maintaining acceptable printability, the crospovidone concentration was increased from 3% to 5% in formulation F17. Printing was successfully completed under the optimized conditions (chamber temperature: 65°C; surface temperature: 95°C), yielding tablets with lower hardness than those produced from F13. Importantly, the tablets remained intact during handling and exhibited no observable powder loss. These results demonstrated that a formulation containing 5% crospovidone and 5% FD&C Red Dye #3, combined with a chamber temperature of

65°C and a surface temperature of 95°C, provided robust printing performance and satisfactory tablet quality.

When formulation F21, containing a higher valsartan loading, was printed using the same optimized conditions, tablet fabrication was successful; however, the resulting tablets were excessively hard and compact. Therefore, formulation F22 was developed by increasing the crospovidone concentration to 7.5% and reducing the surface temperature to 90°C while keeping all other processing parameters unchanged. The tablets produced from F22 exhibited reduced hardness and lower compactness compared with those obtained from F21. Based on their favorable printing characteristics and physical properties, formulations F17 and F22 were selected for further characterization and evaluation. As shown in Table 6, average tablet weights for F17 (275 ± 4.9 mg) and F22 (376 ± 10.2 mg) were close to their target weights of 280 mg and 380 mg respectively.

Single Punch Compressed Tablets

Single-punch compressed tablets were prepared as a reference formulation in a single dosage form for direct comparison with the 3D-printed tablets. To better approximate the characteristics of tablets produced by SLS 3D printing, the lowest feasible compression force was targeted. A minimum compression forces of 1000 psi was required to form intact tablets using the single-punch press. Average tablet weights (Table 6) for all the compressed tablet formulations were close to the target tablet weight of 380 mg.

Drug Content Determination

To determine drug content, three tablets from each formulation (3D-printed and compressed tablets) were individually analyzed using the HPLC method described previously. The drug content and average tablet weight of the 3D-printed and conventionally compressed tablet formulations are presented in Table 6. Overall, all formulations demonstrated acceptable drug loading, with measured contents generally close to the target values for hydrochlorothiazide, valsartan, and amlodipine besylate.

Among the 3D-printed formulations, F17 exhibited drug contents of 101.3 ± 5%, 98.5 ± 3%, and 85.7 ± 1.7% for hydrochlorothiazide, valsartan, and amlodipine besylate, respectively, with an average tablet weight of 275 ± 4.9 mg. While hydrochlorothiazide and valsartan contents were close to the theoretical values, the amlodipine besylate content was lower than expected, suggesting reduced assay recovery or content variability for this drug within the formulation.

Formulation F22, which contained a higher valsartan loading, showed drug contents of 95.0 ± 1.7%, 86.8 ± 0.8%, and 96.7 ± 5.0% for hydrochlorothiazide, valsartan, and amlodipine besylate, respectively. The average tablet weight was 376 ± 10.2 mg. Compared with F17, F22 exhibited lower valsartan recovery but improved amlodipine besylate content. The higher tablet weight observed for F22 was consistent with its increased drug load.

The compressed tablet formulations (F23–F25) demonstrated drug contents close to the target values for all three active pharmaceutical ingredients. Formulation F23 exhibited contents of 100.92 ± 2.6% for hydrochlorothiazide, 104.08 ± 2.5% for valsartan, and 93.78 ± 4.86% for amlodipine besylate, with an average tablet weight of 377.17 ± 4.14 mg. Similarly, F24 showed drug contents of 101.79 ± 2.9%, 112.74 ± 6.3%, and 94.35 ± 3.1% for hydrochlorothiazide, valsartan, and amlodipine besylate, respectively, and an average tablet weight of 379.6 ± 9.2 mg. Formulation F25 exhibited drug contents of 97.88

± 3.9%, 102.16 ± 5.3%, and 92.5 ± 5.4% for hydrochlorothiazide, valsartan, and amlodipine besylate, respectively, with an average tablet weight of 386.1 ± 5.9 mg.

Table 6 Percent assay of 3D printed and compressed multi-drug tablets

Formulation	Hydrochlorothiazide (%w/w)	Valsartan (%w/w)	Amlodipine besylate (%w/w)	Average Tablet Weight (mg)
F17 3D printed	101.3 ± 5.0	98.5 ± 3.0	85.7 ± 1.7	275 ± 4.9
F22 3D printed	95 ± 1.7	86.8 ± 0.8	96.7 ± 5	376 ± 10.2
F23 Compressed	100.92 ± 2.6	104.08 ± 2.5	93.78 ± 4.86	377.17 ± 4.14
F24 Compressed	101.79 ± 2.9	112.74 ± 6.3	94.35 ± 3.1	379.6 ± 9.2
F25 Compressed	97.88 ± 3.9	102.16 ± 5.3	92.5 ± 5.4	386.1 ± 5.9

Drug Dissolution

The in vitro dissolution profiles of hydrochlorothiazide, valsartan, and amlodipine besylate from the optimized 3D-printed formulations F17 and F22 are presented in Fig. 8A and Fig. 8B, respectively.

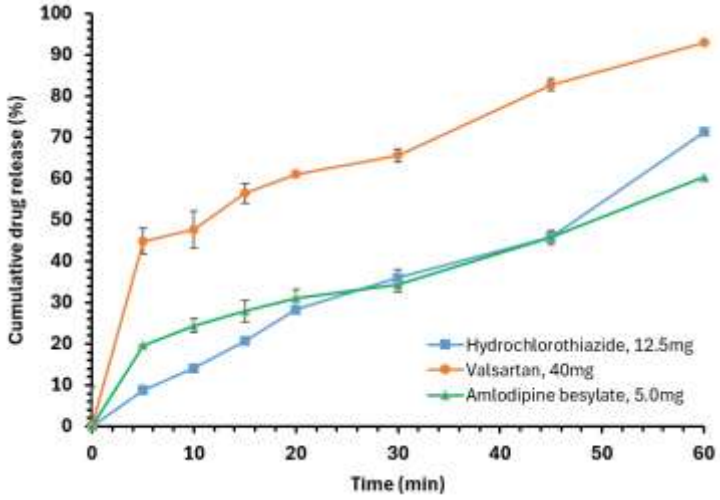

(A)

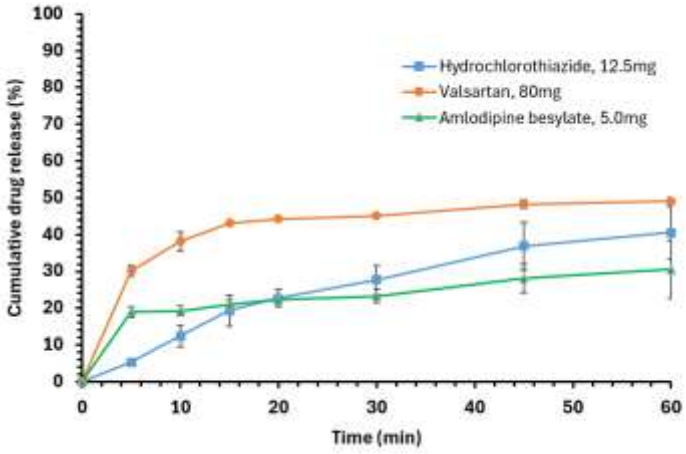

(B)

Figure 8 Drug release profiles from SLS 3D printed tablets at 37 ^{0}C (data presented as mean ± SD, n = 6). Cumulative drug release from (A) Formulation F17, and (B) Formulation F22.

Formulation F17 exhibited the most rapid release of valsartan, with approximately 45% of the drug released within 5 min, increasing to 61% at 20 min and reaching 92.8% after 60 min. In contrast, hydrochlorothiazide and amlodipine besylate showed slower release rates. Hydrochlorothiazide release increased gradually from 8.6% at 5 min to 35.7% at 30 min, reaching 70.9% at 60 min. Similarly, amlodipine besylate exhibited an initial release of 19.3% at 5 min, followed by a gradual increase to 45.4% at 45 min and 60.0% at 60 min. Overall, the release rate from F17 followed the order: valsartan > hydrochlorothiazide > amlodipine besylate at the end of the dissolution period.

The dissolution behavior of formulation F22 differed considerably from that of F17. Although valsartan again showed the fastest initial release, the overall extent of drug release was markedly lower. Approximately 29.9% of valsartan was released within 5 min, increasing to 44.7% at 30 min and reaching only 48.9% after 60 min. Hydrochlorothiazide exhibited a gradual increase in release from 5.0% at 5 min to 27.4% at 30 min, culminating in 40.1% release at 60 min. Amlodipine besylate displayed the slowest dissolution profile, with drug release increasing from 18.4% at 5 min to 23.0% at 30 min and 30.2% at 60 min.

The dissolution profiles of hydrochlorothiazide, valsartan, and amlodipine besylate from compressed tablet formulations F23, F24, and F25 are presented in Figs. 8A, 8B and 9 respectively. The three formulations exhibited distinct release characteristics, with valsartan showing the most rapid and extensive drug release, whereas amlodipine besylate demonstrated the slowest dissolution in all formulations.

Formulation F23 exhibited a gradual release of hydrochlorothiazide, reaching approximately 14.5% at 20 min, 26.2% at 30 min, 45.6% at 60 min, and 72.5% after 120 min. In contrast, valsartan displayed rapid dissolution, with approximately 61.0% of the drug released within 20 min and 86.0% released at 30 min. Nearly complete release was achieved by 45 min (99.3%), reaching 102.6% at 60 min. Amlodipine besylate exhibited a markedly slower release profile, increasing gradually from 8.9% at 15 min to only 13.1% at 120 min. These results demonstrate a pronounced difference in dissolution behavior among the three active pharmaceutical ingredients, with valsartan exhibiting the fastest release from the F23 matrix.

A different release pattern was observed for formulation F24. Hydrochlorothiazide release was enhanced compared with F23, reaching approximately 20.4% at 20 min, 54.6% at 45 min, 75.3% at 60 min, and 90.5% at 120 min. Valsartan again showed rapid dissolution, increasing from 31.4% at 15 min to 84.6% at 45 min and 93.7% at 120 min. Amlodipine besylate demonstrated greater release from F24 than from F23, reaching 25.6% at 45 min, 33.8% at 60 min, and 38.8% at 120 min. Among the three compressed formulations, F24 provided the highest overall release of hydrochlorothiazide and amlodipine besylate.

Formulation F25 produced the most rapid valsartan dissolution profile. More than 100% of valsartan was released within the first 5 min, and the drug release remained essentially constant throughout the study period, indicating immediate and complete dissolution. Hydrochlorothiazide release increased steadily from 21.1% at 5 min to 37.5% at 30 min, 56.0% at 60 min, and 83.2% at 120 min. Similar to F23, amlodipine besylate exhibited limited dissolution, reaching approximately 10.8% at 30 min, 14.6% at 60 min, and 18.1% at 120 min.

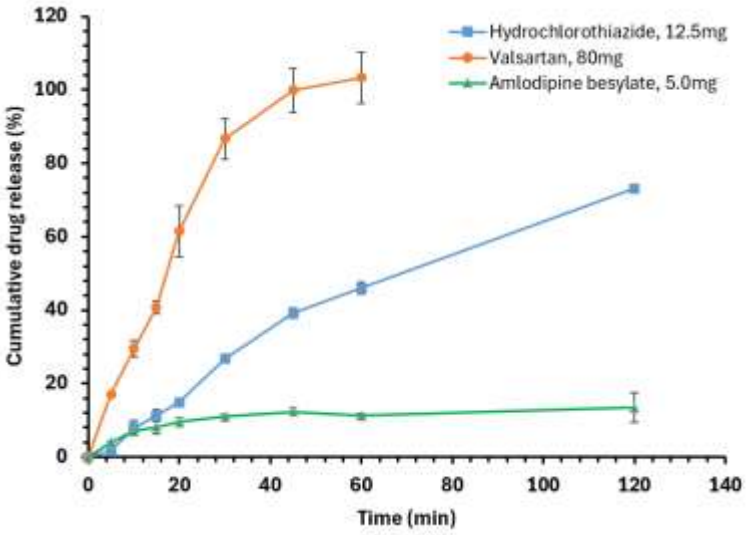

(A)

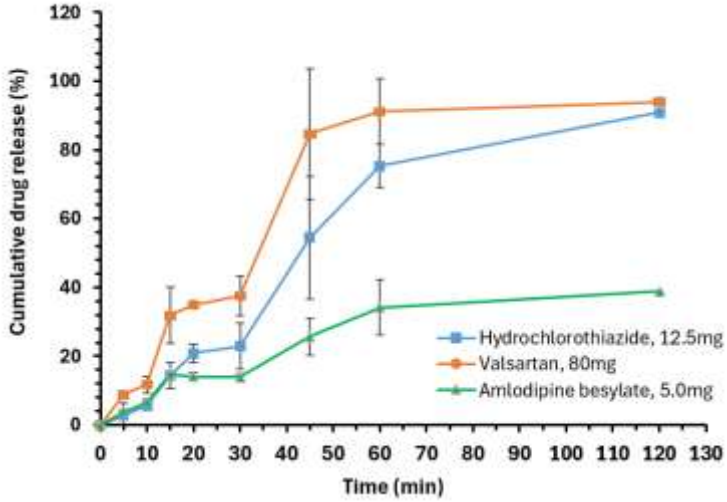

(B)

Figure 8 Drug release profiles from compressed tablets at 37 ^{0}C (data presented as mean ± SD, n = 6). Cumulative drug release from (A) Formulation F23, and (B) Formulation F24.

Comparison of the three compressed formulations revealed notable differences in the release behavior of hydrochlorothiazide and amlodipine besylate. Formulation F24 demonstrated the highest release of both drugs, achieving approximately 90.5% hydrochlorothiazide and 38.8% amlodipine besylate release after 120 min.

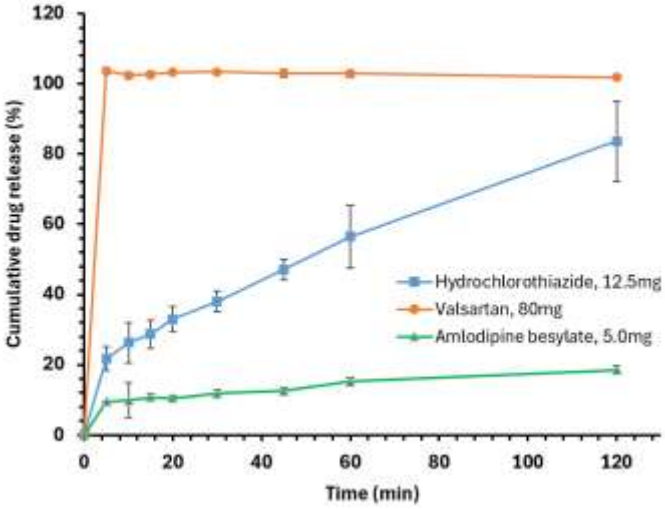

Figure 9 Drug release profile from compressed tablets at 37 ^{0}C from formulation F25(data presented as mean ± SD, n = 6).

In contrast, formulations F23 and F25 exhibited lower amlodipine besylate dissolution, with final releases of approximately 13.1% and 18.1%, respectively. Valsartan release was rapid and extensive in all formulations, with F23 and F25 achieving near-complete dissolution within 60 min, whereas F24 reached approximately 93.7% release after 120 min.

DISCUSSION

Three-dimensional (3D) printing has emerged as a promising manufacturing platform for personalized medicines, enabling the production of dosage forms with patient-specific strengths, drug combinations, and release characteristics. Among the available additive manufacturing technologies, selective laser sintering (SLS) offers several advantages for pharmaceutical applications, including solvent-free processing, single-step fabrication, high printing precision, rapid production, and the ability to manufacture complex dosage forms while minimizing drug degradation. These attributes have established SLS as one of the most promising technologies for personalized oral drug delivery systems [48, 49].

Preformulation studies demonstrated that all investigated excipients were compatible with hydrochlorothiazide, valsartan, and amlodipine besylate, with the exception of mannitol. Thermal analysis revealed a decrease in melting temperature and broadening of melting endotherms when mannitol was combined with hydrochlorothiazide or amlodipine besylate, suggesting potential solid-state interactions. Mannitol has previously been reported to influence drug stability through crystallization-induced changes in water activity within amorphous regions of formulations, which can promote degradation of susceptible drug substances [50-53]. Consequently, mannitol was excluded from further formulation development. Because successful SLS printing requires a thermally responsive excipient capable of promoting particle fusion below the degradation temperatures of the incorporated drugs, Kollidon® VA 64 was selected as the primary binder. The melting temperature of Kollidon® VA 64 (~91°C) was lower than those of hydrochlorothiazide, amlodipine besylate, and valsartan, making it suitable for facilitating laser-induced fusion while minimizing drug degradation. Similar use of copovidone-based polymers in SLS printing has

been reported previously due to their excellent printability and binding characteristics [54, 55].

A gradient HPLC method capable of simultaneously quantifying hydrochlorothiazide, valsartan, and amlodipine besylate was successfully developed. Initial attempts based on published methods [31, 33, 36, 56] were unable to achieve adequate separation because of the considerable differences in physicochemical properties and USP analytical conditions for the three drugs. The optimized gradient method employed a more aqueous initial mobile phase to facilitate elution of the hydrophilic hydrochlorothiazide, followed by an increase in organic content to elute the more lipophilic valsartan and amlodipine besylate. This approach enabled reliable quantification of all three drugs in a single analytical run.

Optimization of SLS process parameters revealed that tablet quality was highly dependent on printing temperature, laser scanning speed, and formulation composition. For placebo tablets, successful fabrication was achieved at a chamber temperature of 95°C, surface temperature of 110°C, and scanning speed of 150 mm/s. Previous studies have shown that laser energy input and scanning speed significantly influence powder fusion, porosity, mechanical strength, and dissolution performance of SLS-printed dosage forms [41, 44, 57]. Consistent with these reports, higher scanning speeds likely reduced the time available for particle fusion, whereas lower speeds promoted more effective sintering and tablet formation.

Although these conditions produced acceptable placebo tablets, formulation F11 could not be printed successfully because the powder blend solidified before proper spreading. DSC analysis revealed an onset melting temperature of 73°C and a melting peak at 88°C, substantially lower than the temperatures used for placebo printing. The reduced thermal transition likely resulted from interactions between valsartan and Kollidon® VA 64, both of which possess relatively low melting temperatures. Adjustment of the chamber and surface temperatures ultimately led to successful fabrication of F13 at 65°C and 95°C, respectively. However, the tablets exhibited excessive hardness and compactness. Increasing crospovidone concentration and maintaining 5% FD&C Red Dye No. 3 yielded formulation F17, which showed acceptable mechanical integrity and handling characteristics. When valsartan loading was increased in F21, tablet hardness increased further, necessitating formulation optimization through higher crospovidone content and a lower surface temperature, resulting in formulation F22.

Drug-content analysis demonstrated acceptable assay values for all formulations, indicating that neither SLS processing nor conventional compression adversely affected drug loading. The assays obtained for the 3D-printed tablets (F17 and F22) and compressed tablets (F23–F25) were within pharmacopeial acceptance limits, confirming the robustness of both manufacturing approaches.

The dissolution studies highlighted substantial differences between the 3D-printed and compressed formulations. Formulation F17 achieved 60-min releases of approximately 71% hydrochlorothiazide, 93% valsartan, and 60% amlodipine besylate, whereas F22 exhibited significantly lower releases of approximately 40%, 49%, and 23%, respectively. The reduced dissolution observed for F22 is likely attributable to its higher valsartan content, which increased matrix densification through enhanced fusion with Kollidon® VA 64 during sintering. SLS processing is known to produce amorphous or partially fused polymeric matrices, and increasing

polymer-drug interactions can reduce porosity and water penetration, thereby slowing drug release [41, 55, 58].

Evidence also suggested that FD&C Red Dye No. 3 contributed to altered dissolution behavior. DSC analysis showed shifts in the valsartan melting endotherm and the appearance of exothermic events for hydrochlorothiazide and amlodipine besylate, indicating possible drug–dye interactions. To explore this hypothesis, single-punch compressed tablets were prepared. Formulation F23, which contained dye but did not undergo thermal processing, showed substantially higher valsartan release than F22, suggesting that thermal fusion between valsartan and Kollidon® VA 64 played a major role in the slower dissolution of the 3D-printed tablets. More importantly, elimination of the dye in F24 resulted in markedly improved release of hydrochlorothiazide and amlodipine besylate, further supporting the possibility of drug–dye interactions affecting dissolution performance. This observation was reinforced by formulation F25. Despite rapid tablet disintegration, attributable to the inclusion of microcrystalline cellulose and sucrose, hydrochlorothiazide and amlodipine besylate still exhibited relatively poor dissolution. If disintegration was the sole limiting factor, improved dissolution would have been expected. Therefore, the persistence of reduced drug release despite rapid tablet breakup suggests that interactions involving FD&C Red Dye No. 3 may have influenced drug solubility or wettability, particularly for hydrochlorothiazide and amlodipine besylate. Additional solid-state characterization techniques such as PXRD, FTIR, Raman spectroscopy, and hot-stage microscopy would be valuable in future studies to elucidate the nature of these interactions.

Overall, the study demonstrates the feasibility of producing variable-dose combination tablets containing hydrochlorothiazide, valsartan, and amlodipine besylate using SLS 3D printing. Printing performance and drug release were strongly influenced by formulation composition and process parameters. Formulation F17 provided the most favorable balance between printability, mechanical strength, drug content uniformity, and dissolution performance. The findings further highlight the importance of excipient selection and excipient-drug interactions in the development of SLS-manufactured multi-drug dosage forms and support the continued application of SLS technology for personalized cardiovascular therapies.

CONCLUSION

This study successfully demonstrated the feasibility of utilizing selective laser sintering (SLS) 3D printing to fabricate personalized multi-drug antihypertensive tablets containing hydrochlorothiazide, valsartan, and amlodipine besylate at variable dose strengths. A novel gradient HPLC method was developed and validated for the simultaneous quantification of all three drugs, providing a robust analytical tool for formulation development and quality assessment.

Preformulation studies established the compatibility of the selected drugs with most investigated excipients, while identifying mannitol as unsuitable because of potential interactions with hydrochlorothiazide and amlodipine besylate. Optimization of formulation composition and printing parameters revealed that successful fabrication of multi-drug tablets depended strongly on thermal properties of the powder blend, dye concentration, and disintegrant level. The optimized formulations (F17 and F22) were successfully printed with acceptable physical characteristics and drug content uniformity,

demonstrating the capability of SLS technology to produce individualized fixed-dose combination products.

Dissolution studies showed that drug release behavior was significantly influenced by formulation composition and processing conditions. Formulation F17 exhibited the most favorable overall performance, achieving substantially higher drug release than F22, while comparison with conventionally compressed tablets highlighted the influence of SLS-induced fusion and potential interactions involving FD&C Red Dye No. 3 on dissolution characteristics. The improved release observed in dye-free compressed tablets suggests that further investigation of dye–drug interactions is warranted to optimize formulation performance.

Overall, the findings demonstrate that SLS 3D printing is a promising platform for the manufacture of personalized cardiovascular polypills capable of delivering multiple antihypertensive agents within a single dosage form. The technology offers flexibility in dose customization, supports the goals of precision medicine, and has the potential to improve patient adherence by reducing pill burden. Future studies should focus on detailed solid-state characterization, optimization of excipient selection, and evaluation of long-term stability and scalable manufacturing approaches to facilitate the clinical translation of personalized SLS-printed multi-drug tablets.

DECLARATION OF COMPETING INTEREST

The authors declare that they have no known competing financial interests or personal relationships that could have appeared to influence the work reported in this paper.

ACKNOWLEDGEMENTS

Financial support for this project was provided by the School of Pharmacy at the Massachusetts College of Pharmacy and Health Sciences as well as Massachusetts Life Sciences Center-Capital Grants.

REFERENCES

1. Oparil, S., et al., Hypertension. Nature Reviews Disease Primers, 2018. 4(1): p. 18014.
2. Oparil, S., et al., Hypertension. Nat Rev Dis Primers, 2018. 4: p. 18014.
3. Oparil, S., M.A. Zaman, and D.A. Calhoun, Pathogenesis of hypertension. Annals of internal medicine, 2003. 139(9): p. 761-776.
4. Mills, K.T., A. Stefanescu, and J. He, The global epidemiology of hypertension. Nat Rev Nephrol, 2020. 16(4): p. 223-237.
5. Borghi, C., et al., Projecting the long-term benefits of single pill combination therapy for patients with hypertension in five countries. Int J Cardiol Cardiovasc Risk Prev, 2021. 10: p. 200102.
6. Nguyen, Q., et al., Hypertension management: an update. Am Health Drug Benefits, 2010. 3(1): p. 47-56.
7. Jneid, H., et al., 2012 ACCF/AHA focused update of the guideline for the management of patients with unstable angina/Non-ST-elevation myocardial infarction (updating the 2007 guideline and replacing the 2011 focused update): a report of the American College of Cardiology Foundation/American Heart Association Task Force on practice guidelines. Circulation, 2012. 126(7): p. 875-910.
8. Elliott, W.J. and C.V.S. Ram, Calcium channel blockers. The Journal of Clinical Hypertension, 2011. 13(9): p. 687.
9. Roush, G.C. and D.A. Sica, Diuretics for hypertension: a review and update. American journal of hypertension, 2016. 29(10): p. 1130-1137.

10. Malachias, M., et al., 7 th Brazilian Guideline of Arterial Hypertension: Chapter 2-Diagnosis and Classification. Arquivos brasileiros de cardiologia, 2016. 107: p. 07-13.
11. Wald, D.S., et al., Combination therapy versus monotherapy in reducing blood pressure: meta-analysis on 11,000 participants from 42 trials. The American journal of medicine, 2009. 122(3): p. 290-300.
12. Mourad, J.-J., et al., Comparison of different therapeutic strategies in hypertension: a low-dose combination of perindopril/indapamide versus a sequential monotherapy or a stepped-care approach. Journal of hypertension, 2004. 22(12): p. 2379-2386.
13. Palatini, P., Combination therapy in the management of hypertension: focus on angiotensin receptor blockers combined with diuretics. J Clin Hypertens (Greenwich), 2005. 7(2): p. 96-101.
14. Weir, M.R. and G.L. Bakris, Combination therapy with Renin-Angiotensin-aldosterone receptor blockers for hypertension: how far have we come? The Journal of Clinical Hypertension, 2008. 10(2): p. 146-152.
15. Kochar, M., et al., Matrix study of irbesartan with hydrochlorothiazide in mild-to-moderate hypertension. American journal of hypertension, 1999. 12(8): p. 797-805.
16. Weir, M.R., Incidence of pedal edema formation with dihydropyridine calcium channel blockers: issues and practical significance. Journal of clinical hypertension (Greenwich, Conn.), 2003. 5(5): p. 330-335.
17. De la Sierra, A., Mitigation of calcium channel blocker-related oedema in hypertension by antagonists of the renin–angiotensin system. Journal of human hypertension, 2009. 23(8): p. 503-511.
18. Burnier, M., Antihypertensive combination treatment: state of the art. Current hypertension reports, 2015. 17: p. 1-9.
19. What is precision medicine? MedlinePlus, 2020.
20. Ginsburg, G.S. and K.A. Phillips, Precision Medicine: From Science To Value. Health Aff (Millwood), 2018. 37(5): p. 694-701.
21. Tan, Y.J.N., et al., Customizable drug tablets with constant release profiles via 3D printing technology. Int J Pharm, 2021. 598: p. 120370.
22. Wening, K. and J. Breitkreutz, Oral drug delivery in personalized medicine: Unmet needs and novel approaches. International Journal of Pharmaceutics, 2011. 404(1): p. 1-9.
23. Cook, T.J., et al., Variability in tablet fragment weights when splitting unscored cyclobenzaprine 10 mg tablets. J Am Pharm Assoc (2003), 2004. 44(5): p. 583-6.
24. Rautamo, M., et al., Benefits and Prerequisites Associated with the Adoption of Oral 3D-Printed Medicines for Pediatric Patients: A Focus Group Study among Healthcare Professionals. Pharmaceutics, 2020. 12(3).
25. Shahrubudin, N., T.C. Lee, and R. Ramlan, An Overview on 3D Printing Technology: Technological, Materials, and Applications. Procedia Manufacturing, 2019. 35: p. 1286-1296.
26. Kalaskar, D.M., 3D printing in medicine. 2022: Woodhead Publishing.
27. Elkasabgy, N.A., A.A. Mahmoud, and A. Maged, 3D printing: An appealing route for customized drug delivery systems. International Journal of Pharmaceutics, 2020. 588: p. 119732.
28. Rautamo, M., et al., Benefits and Prerequisites Associated with the Adoption of Oral 3D-Printed Medicines for Pediatric Patients: A Focus Group Study among Healthcare Professionals. Pharmaceutics, 2020. 12.
29. Tan, Y.J.N., et al., On-demand fully customizable drug tablets via 3D printing technology for personalized medicine. J Control Release, 2020. 322: p. 42-52.
30. Basit, A.W., 3D printing of pharmaceuticals and the role of pharmacy. The Pharmaceutical Journal, 2022.
31. United States Pharmacopoeia. USP43-NF38. p 4577.
32. Çelebier, M., et al., HPLC method development for the simultaneous analysis of amlodipine and valsartan in combined dosage forms and in vitro dissolution studies.

Brazilian Journal of Pharmaceutical Sciences, 2010. 46: p. 761-768.
33. Kruth, J.-P., et al., Consolidation phenomena in laser and powder-bed based layered manufacturing. CIRP annals, 2007. 56(2): p. 730-759.
34. United States Pharmacopoeia. USP43-NF38. p. 4580.
35. United Stated Pharmacopoeia. USP43-NF38. p. 285.
36. United States Pharmacopoeia. USPNF 2022 ISSUE 1 - Online.
37. Hydrochlorothiazide (Rx).
38. Valsartan (Rx).
39. Amlodipine (Rx).
40. Amlodipine, Valsartan, and Hydrochlorothiazide Tablets, in United States Pharmacopoeia. p. USP43-NF38 - 279.
41. Awad, A., et al., 3D printing: Principles and pharmaceutical applications of selective laser sintering. International Journal of Pharmaceutics, 2020. 586: p. 119594.
42. Allahham, N., et al., Selective Laser Sintering 3D Printing of Orally Disintegrating Printlets Containing Ondansetron. Pharmaceutics, 2020. 12(2).
43. Awad, A., et al., 3D Printed Tablets (Printlets) with Braille and Moon Patterns for Visually Impaired Patients. Pharmaceutics, 2020. 12(2).
44. Barakh Ali, S.F., et al., Understanding the effects of formulation and process variables on the printlets quality manufactured by selective laser sintering 3D printing. Int J Pharm, 2019. 570: p. 118651.
45. Mohamed, E.M., et al., Formulation Optimization of Selective Laser Sintering 3D-Printed Tablets of Clindamycin Palmitate Hydrochloride by Response Surface Methodology. AAPS PharmSciTech, 2020. 21(6): p. 232.
46. Tabriz, A.G., et al., 3D Printing of Personalised Carvedilol Tablets Using Selective Laser Sintering. Pharmaceutics, 2023. 15(9).
47. Zarmpi, P., et al., Biopharmaceutical aspects and implications of excipient variability in drug product performance. Eur J Pharm Biopharm, 2017. 111: p. 1-15.
48. Fina, F., et al., 3D printing of drug-loaded gyroid lattices using selective laser sintering. International journal of pharmaceutics, 2018. 547(1-2): p. 44-52.
49. Shirazi, S.F.S., et al., A review on powder-based additive manufacturing for tissue engineering: selective laser sintering and inkjet 3D printing. Science and technology of advanced materials, 2015.
50. Arte, K.S., et al., Understanding the impact of mannitol on physical stability and aerosolization of spray-dried protein powders for inhalation. International Journal of Pharmaceutics, 2024. 650: p. 123698.
51. de Oliveira, M.A., M.I. Yoshida, and D.C. Silva, Quality evaluation of pharmaceutical formulations containing hydrochlorothiazide. Molecules, 2014. 19(10): p. 16824-36.
52. Kosugi, A., et al., Effect of Different Direct Compaction Grades of Mannitol on the Storage Stability of Tablet Properties Investigated Using a Kohonen Self-Organizing Map and Elastic Net Regression Model. Pharmaceutics, 2020. 12(9): p. 886.
53. Shaikh, J.S.A., et al., High performance liquid chromatographic assay of amlodipine, valsartan and hydrochlorothiazide simultaneously and its application to pharmaceuticals, urine and plasma analysis. J Chromatogr B Analyt Technol Biomed Life Sci, 2020. 1155: p. 122295.
54. Fina, F., et al., Fabricating 3D printed orally disintegrating printlets using selective laser sintering. Int J Pharm, 2018. 541(1-2): p. 101-107.
55. Gueche, Y.A., et al., Selective Laser Sintering of Solid Oral Dosage Forms with Copovidone and Paracetamol Using a CO(2) Laser. Pharmaceutics, 2021. 13(2).
56. Ares, A. and J. Bernal, Hydrophilic interaction chromatography in drug analysis. Open Chemistry, 2012. 10(3): p. 534-553.
57. Balasankar, A., et al., Recent Advances in the Production of Pharmaceuticals Using Selective Laser Sintering. Biomimetics (Basel), 2023. 8(4).

58. Fina, F., et al., Selective laser sintering (SLS) 3D printing of medicines. Int J Pharm, 2017. 529(1-2): p. 285-293.

HOW TO CITE: Sanjaykumar Gayakwad, Alisha Patel, Development of 3D Printed Variable Dose Multi-Drug Tablets Containing Metformin, Sitagliptin, and Simvastatin by Selective Laser Sintering and their Simultaneous Quantification Using a Novel HPLC Method, Int. J. of Pharm. Sci., 2026, Vol 4, Issue 8, 609-632. https://doi.org/10.5281/zenodo.21800558